Solitary waves associated with Short Large-Amplitude Magnetic Structures (SLAMS) upstream of the Earth's quasi-parallel bow shock

R. Behlke[1,2], M. André[1], S.D. Bale[3], J.S. Pickett[4], C.A. Cattell[5], E.A. Lucek[6], A.N. Fazakerley[7], and A. Balogh[6]

Abstract. For the first time, solitary waves (SWs) have been observed within Short Large-Amplitude Magnetic Structures (SLAMS) upstream of the Earth's quasi-parallel bow shock. They occur as bipolar (at times tripolar) pulses together with wave packets. These nonlinear structures are consistent with electron holes propagating parallel to the magnetic field with velocities of the order of 100's km/s and amplitudes up to 65 mV/m. The solitary waves have scale sizes comparable to the Debye length and represent positive potential structures with potentials of the order of 1 V. Solitary waves are suggested to play an important role in dissipation within SLAMS.

1. Introduction

The character of collisionless shocks is determined by the angle θ_{Bn} between the upstream magnetic field and the nominal shock normal. At the Earth's quasi-parallel bow shock, so-called Short Large-Amplitude Magnetic Structures (SLAMS) are commonly observed (Schwartz et al., 1992; Lucek et al., 2002; Behlke et al., 2003). Observations (Schwartz et al., 1992) combined with simulations (Burgess, 1989) led to the model of a shock, which is cyclically reforming and built up of a patchwork of SLAMS (Schwartz and Burgess, 1991). The quasi-parallel shock could thus be described as an extended transition region characterised by the growth, deceleration and merging of SLAMS rather than a single, two-dimensional surface.

Solitary waves (SWs) travelling parallel to the background magnetic field have been reported from various parts of the magnetosphere. They are characterized by their bipolar electric field structure parallel to the magnetic field. SWs were first observed in the auroral acceleration region by S3-3 (Temerin et al., 1982). They are found at narrow boundaries, such as the plasma sheet boundary (Matsumoto et al., 1994; Cattell et al., 1998) and the quasi-perpendicular bow shock (Bale et al., 1998; Bale et al., 2002) and in regions with strong currents, such as the auroral acceleration region (Temerin et al., 1982; Boström et al., 1988; Mozer et al., 1997). Observations of SWs were also reported from the solar wind (Mangeney et al., 1999), the high altitude polar cap boundary (Tsurutani et al., 1998), at high altitude cusp injections (Cattell et al., 2001) and the magnetopause (Cattell et al., 2002). In most cases, the observations were identified as electron solitary waves. They are observed at both high and low altitudes for a wide range of $f_{\rm ce}/f_{\rm pe}$. However, ion solitary waves have so far only been reported from the low altitude auroral region where $f_{\rm ce}/f_{\rm pe} \gg 1$ (Bounds et al., 1999; Crumley et al., 2001; Dombeck et al., 2001). In this letter, we present the first observations, as known to the authors, of solitary structures within SLAMS.

The data for this study were obtained by the Electric Field and Wave (EFW) experiment (Gustafsson et al., 1997) onboard the four Cluster spacecraft (Escoubet et al., 1997). The EFW experiment consists of two pairs of spherical probes on wire booms in the spin plane of each satellite (approximately the ecliptical plane). The separation between each probe pair is 88 m. For the data presented here, the probe potential with respect to the spacecraft is sampled both at 32,000 samples per second using a lowpass filter at 9 kHz (internal burst mode data rate, called IBM hereafter), as well as at 5 samples per second (normal mode data rate, called NM hereafter). This measurement is usually referred to as the negative spacecraft potential $-v_{sp}$ and gives an estimate of the plasma density (Pedersen et al., 2001). Furthermore, data from the fluxgate magnetometer (FGM), see Balogh et al. (2001), are used for the idenfication of SLAMS.

2. Observations

An example of a quasi-parallel bow shock crossing on February 3, 2002, at $\sim$(12, 3, -8) R_E (in GSE) is presented in Figure 1. The transition from the solar wind (UT 04:30-04:50) to a more turbulent region (from UT 04:50) with magnetic field and density pulsations can clearly be seen in panels (a)-(b) which display $-v_{sp}$ and the magnetic field magnitude B, respectively. In panels (c)-(e), a shorter interval of 1 min (UT 04:59:20-05:00:20) reveals typical signatures of Short Large-Amplitude Magnetic Structures (SLAMS). They are characterized by density enhancements (Behlke et al., 2003), as seen in panel (c), as well as magnetic field enhancements (Schwarz et al., 1992), as seen in panel (d). SLAMS are typically associated with rotations of the magnetic field (Mann et al., 1994), see panel (e) which plots

[1]Swedish Institute of Space Physics, Uppsala division, Uppsala, Sweden.
[2]Department of Astronomy and Space Physics, Uppsala University, Uppsala, Sweden.
[3]Space Sciences Laboratory, University of California, Berkeley, USA.
[4]Department of Physics and Astronomy, University of Iowa, Iowa City, USA.
[5]School of Physics and Astronomy, University of Minnesota, Minneapolis, USA.
[6]Blackett Laboratory, Imperial College, London, UK.
[7]Mullard Space Science Laboratory, University College London, UK.

Paper number .
0094-8276/03/$5.00

the magnetic field elavation θ_B. Although all four Cluster spacecraft were recording data during this period, we only present data for one spacecraft in this plot. Firstly, IBM data are only recorded for one satellite at a time. Secondly, the plot is restricted to one spacecraft for clarity reasons, since panels (c)-(e) are nearly identical during this event at $\sim$ 100 km separation. For multi-spacecraft observations of SLAMS, see Lucek et al. (2002) and Behlke et al. (2003). A zoom-in of panels (c)-(e) is shown in panel (f) displaying an interval of 11.5 sec during which an EFW internal burst was recorded. The black circles give the NM data whereas the red line shows the IBM data for probe 2. During this interval, two SLAMS are observed at UT 04:59:35 and 04:59:42.

Note that some features of the SLAMS are only visible in the IBM data. Firstly, the right-hand side of the SLAMS (i.e., the leading edge; the solar wind comes from the right-hand side) around UT 04:59:35 appears much steeper in the IBM data than in the NM data, additionally exhibiting an over-shoot-like feature. Earlier observations of SLAMS with longer duration (around 15 sec) already revealed the feature of a steepened leading edge, but did not show overshoot-like characteristics (Lucek et al., 2002; Behlke et al., 2003). Observations of quasi-perpendicular shock crossings commonly display an overshoot. Secondly, short-duration, high-amplitude spikes as well as high-frequency wave packets can be observed in the IBM data. The latter group will be subject of this study. During this quasi-parallel shock crossing, two more internal burst modes have been recorded adding upp to a total of about 33 sec of high-resolution data.

Note that the pattern of vertical lines in panel (f) around UT 04:59:44 is due to the active sounding of the WHISPER instrument onboard Cluster.

Figure 2 shows two short intervals of 15 msec with IBM data for spacecraft 4. E_{12} is defined as the difference of the negative probe to spacecraft potential for probe 1 and 2, divided by the probe separation of $l = 88$ m, i.e., $E_{12} = (p1 - p2)/l$. E_{34} is defined correspondingly for probe 3 and 4. The notation of the probes is such that probes 1 & 2 and 3 & 4 lie oppposite to each other. We use E_{12} and E_{34} instead of the single probe measurements in order to exclude the spacecraft potential, whose influence on the measurements is difficult to quantify. Panels (a)-(b) display an example of typical bipolar structures observed within SLAMS. They have durations $\Delta t \leq 1$ msec and top-to-top amplitudes $E' \leq 10$ mV/m. During this interval, $\theta_B \sim 30°$. Several spikes are embebbed in a weaker nonlinear wave

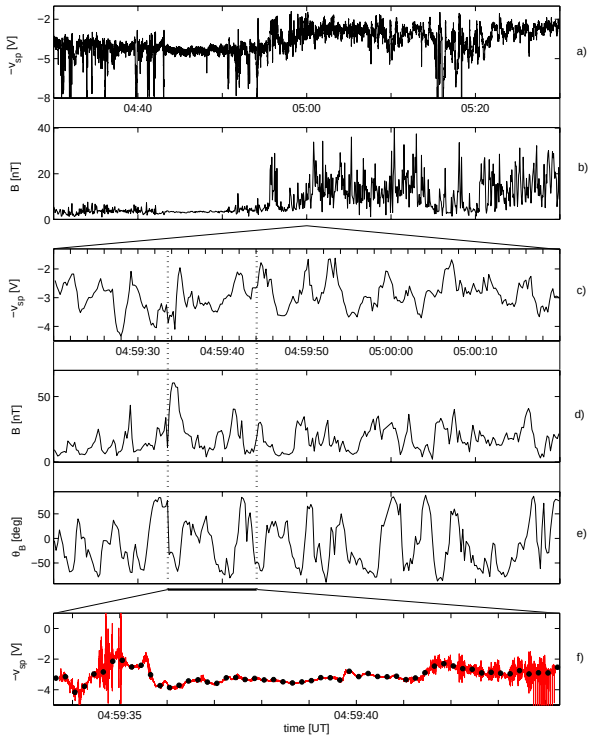

Figure 1. Observations by Cluster satellite 4 on February 3, 2002. Note the different time intervals for panels (a)-(b), (c)-(e) and (f), respectively. Panel (a) shows the negative spacecraft potential $-v_{sp}$ for UT 04:30-05:30. This parameter is correlated with the plasma density, i.e., high $-v_{sp}$ corresponds to a high density (e.g., a $-v_{sp}$ of -8, -5, -2 V corresponds to about 6, 20, 100 particles cm^{-3}). Panel (b) displays the magnetic field magnitude B from FGM for the same period. Panels (c)-(e) show 1 min of data (UT 04:59:20-05:00:20) of the negative spacecraft potential $-v_{sp}$, the magnetic field magnitude B and the elevation angle of the magnetic field θ_B, respectively. Here, $\theta_B = 90°$ corresponds to a strictly northward field. Panel (f) displays 11.5 sec of data (UT 04:59:33.6-04:59:45.1) for probe 2. The red line gives the IBM data (32 kHz sampling rate) with NM data (5 Hz sampling rate) overlayed as black circles.

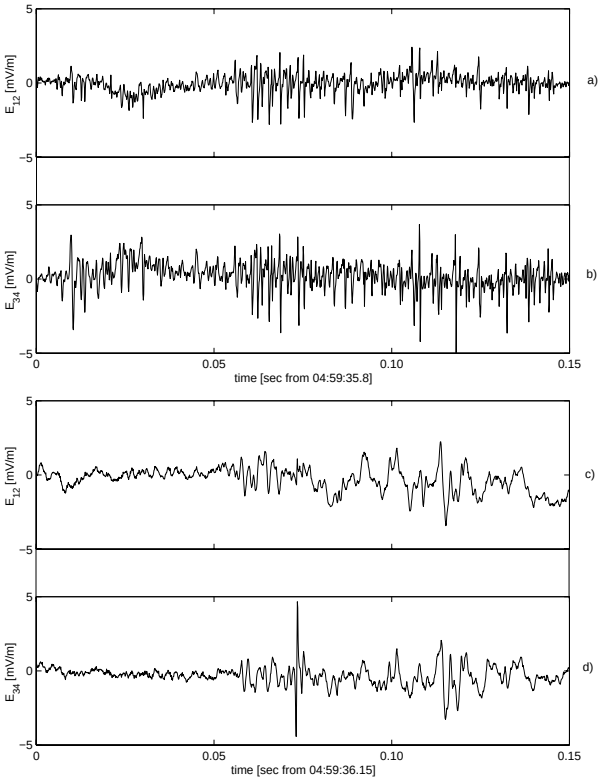

Figure 2. Observations by Cluster 4 on February 3, 2002. Panels (a)-(b) display E_{12} and E_{34} (definition see text) with start at UT 04:59:35.8. This period contains common bipolar signatures appearing in groups within a SLAMS (here $\theta_B \sim 30°$). They have amplitudes E' up to 9 mV/m and durations Δt of 1 msec. Panels (c)-(d) give E_{12} and E_{34} with start at UT 04:59:36.15. Here, a single bipolar structure within a SLAMS is shown with $\theta_B \sim 0°$.

field. Solitary waves (SWs) are structures characterized by a bipolar electric field pulse parallel to the background magnetic field. To determine the physical structure of a SW, its velocity vector must be determined. This can be done using the four probes as an interferometer when $\theta_B \sim 0^\circ$. The procedure is described in detail by Dombeck et al. (2001). Panels (c)-(d) give an example of a SW with $\theta_B \sim 0^\circ$. The magnetic field is nearly aligned with probe pair 34 (within a few degrees). The analysis for this SW yields a velocity of $v \sim 400$ km/s and a unipolar potential (integrated over the parallel component over the structure) of $\Phi_{\|} = 0.8$ V. The duration of the pulse is $\Delta t \sim 1$ msec, which gives a parallel scale length $L_{\|} \sim 400$ m. This is of the order of the Debye length under these conditions ($\lambda_D \sim 1$ km). The analysis of other SWs with $\theta_B \sim 0^\circ$ yields similar results.

Figure 3 shows other classes of signatures than presented in Figure 2. Panels (a)-(b) display E_{12} and E_{34} for a period of 0.1 sec within the SLAMS. These structures are of longer duration ($\Delta t \sim 5$ msec) and higher amplitudes ($E' \sim 65$ mV/m). Since $\theta_B \sim -35^\circ$, we cannot obtain a reliable estimate of the speed and thus the scale and potential of these structures. Panels (c)-(d) show that bipolar structures are not only confined to SLAMS, but can also be found outside of SLAMS, here upstream of a SLAMS ($\theta_B \sim -30^\circ$). These are similar to the common features within SLAMS in terms of duration and amplitudes.

Figure 4 presents yet two more classes of signatures within SLAMS. Panels (a)-(b) show the signature of a tripolar structure with $\Delta t \sim 6$ msec and $E' \sim 23$ mV/m ($\theta_B \sim 55^\circ$). Observations of similar structures have been reported in the literature. Panels (c)-(d) give an example of a large-amplitude ($E'_{\max} = 62$ mV/m) and high-frequency ($f \sim 630$ Hz) wave packet for $\theta_B \sim -60^\circ$, commonly observed in the IBM data within SLAMS.

3. Discussion and Conclusions

We have reported on the first observations of nonlinear, electric field pulses (solitary waves) associated with Short Large-Amplitude Magnetic Structures (SLAMS) upstream of the Earth's quasi-parallel bow shock. The SWs have amplitudes up to 65 mV/m and velocities of a few 100 km/s. The scale sizes are of the order of 1 km, which is comparable to the Debye length for the range of plasma conditions within SLAMS. Almost all observed SWs are positive potential structures with potentials of the order of 1 V. Positive potential SWs with velocities of 100's of km/s are consistent with electron phase space holes (Muschietti et al., 1999) which propagate at a speed comparable to the electron thermal speed.

The potential of the SWs can be compared with the cross-shock potential over a single SLAMS. Generally, the four Cluster spacecraft can be used to determine the speed and normal vector of a SLAMS. The electric field measured by the EFW instrument can then be transformed in the shock

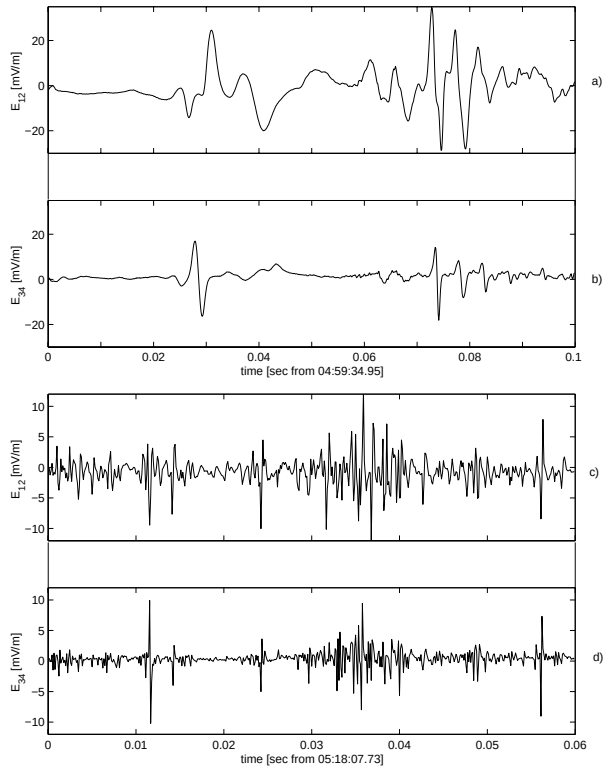

Figure 3. Observations by Cluster 3 and 4 on February 3, 2002. Panels (a)-(b) display E_{12} and E_{34} for spacecraft 4 with start at UT 04:59:34.95. Here, rather different signatures, compared to Figure 2, with $E' \sim 65$ mV/m and $\Delta t \sim 5$ msec are shown ($\theta_B \sim -35^\circ$). Panels (c)-(d) show E_{12} and E_{34} for spacecraft 3 with start at UT 05:18:07.73. This period upstream of a SLAMS contains bipolar signatures comparable to those in Figure 2, but with higher $E' \sim 20$ mV/m ($\theta_B \sim -30^\circ$).

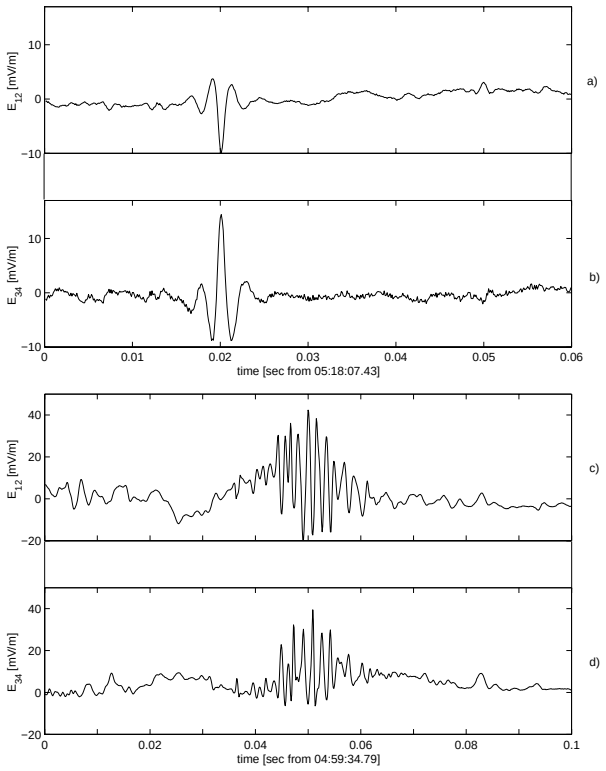

Figure 4. Observations by Cluster 3 and 4 on February 3, 2002. Panels (a)-(b) display E_{12} and E_{34} for spacecraft 3 with start at UT 05:18:07.43. This period contains an example of rather rare tripolar structures within SLAMS with $E' \sim 23$ mV/m and $\Delta t \sim 6$ msec ($\theta_B \sim 55^\circ$). Panels (c)-(d) show E_{12} and E_{34} for spacecraft 4 with start at UT 04:59:34.79. This is an example of an high-frequency wave packet within SLAMS with $f \sim 630$ Hz and $E'_{\max} \sim 62$ mV/m ($\theta_B \sim -60^\circ$).

frame moving with the SLAMS and thereafter in the Normal Incident Frame (NIF), in which is the incoming solar wind is parallel to the SLAMS' normal vector. Integration over the normal vector of the electric field in the NIF yields then the cross-shock potential. The procedure is described for quasi-perpendicular shock crossings by Balikhin et al. (2002). SLAMS usually have a cross-shock potential of the order of a few 100 V up to 1000 V. Browsing the data within a single SLAMS yields 100's of solitary structures. Using a mean potential over a SW of the order of 1 V adds up to 100's of Volts. This suggests that solitary structures provide a small, but significant, contribution to the all-over cross-shock potential associated with SLAMS and might thus play a role in particle acceleration or dissipation at SLAMS. SLAMS in their turn are thought to build up the quasi-parallel bow shock and answer for the dissipation over the shock transition region. Large-amplitude, high-frequency wave packets containing a net potential might add to the potential over the SWs. These processes are not well-understood and require further investigation.

Simulations of electron phase space holes (EH's) by Omura et al. (1996) and Goldman et al. (1999), as well as references therein, showed that they strongly interact with particles which results in particle trapping and heating. Carlson et al. (1998) presented simulations and observations of electron phase space holes in the auroral zone and showed that electron holes lead to energy transfer between electron and ions. However, SWs within SLAMS produce smaller amplitudes than elsewhere in the magnetosphere ($|E| > 1000$ mV/m). Still, they may play an important role in processes, such as dissipation, because EH's occur in large numbers and even small amplitude holes dramatically affect the electron distribution.

Further studies on SWs within SLAMS need to include statistics on scale lengths and potential of SWs. A further issue is the understanding and association between SWs of different shapes, durations and scales. Observations with the Wideband (WBD) plasma investigation (Gurnett et al., 1997) onboard Cluster suggest yet a further class of SWs with durations of the order of 10's of microseconds.

References

Bale, S.D., et al., Bipolar electrostatic structures in the shock transition region: Evidence of electron phase space holes, *Geophys. Res. Lett., 15*, 2929–2932, 1998.

Bale, S.D., et al., Electrostatic turbulence and Debye-scale structures associated with electron thermalization at collisionless shocks, *Ap. J., 575*, L25–L28, 2002.

Balikhin, M.A., et al., Observation of the terrestrial bow shock in quasi-electrostatic subshock regime, *J. Geophys. Res., 107*(A8), 10.1029/2001JA000327, 2002.

Balogh, A., et al., The Cluster Magnetic Field Investigation: Overview of in-flight performance and initial results, *Ann. Geophys., 19*, 1207–1217, 2001.

Behlke, R., et al., Multi-point electric field measurements of Short Large-Amplitude Magnetic Structures (SLAMS) at the Earth's quasi-parallel bow shock, *Geophys. Res. Lett., 30*(4), 10.1029/2002GL015871, 2003.

Boström, R., et al., Characteristics of solitary waves and weak double layers in the magnetospheric plasma, *Phys. Rev. Lett., 61*, 82–85, 1988.

Bounds, S.R., et al., Solitary potential structures associated with ion and electron beams near 1 R_E altitude, *J. Geophys. Res., 104*, 28709, 1999.

Burgess, D., Cyclic behaviour at quasi-parallel collisionless shocks, *Geophys. Res. Lett., 16*, 345–348, 1989.

Carlson, C.W., et al., NEED TO CHECK THIS OUT !!!

Cattell, C.A., et al., Observations of large amplitude parallel electric field wave packets at the plasma sheet boundary, *Geophys. Res. Lett., 26*, 857–860, 1998.

Cattell, C.A., et al., POLAR observations of solitary waves at high and low altitudes and comparison to theory, *Adv. Space Res., 28*, 1631–1641, 2001.

Cattell, C.A., et al., POLAR observations of solitary waves at the Earth's magnetopause, *Geophys. Res. Lett., 29*(5), 9:1–9:4, 10.1029/2001GL014046, 2002.

Crumley, J.P., et al., Studies of ion solitary waves using simulations including hydrogen and oxygen beams, *J. Geophys. Res., 106*, 6007–6015, 2001.

Dombeck, J., et al., Observed trends in auroral zon ion mode solitary wave structure characteristics using data from Polar, *J. Geophys. Res., 106*, 19013–19021, 2001.

Escoubet, C.P., et al., Cluster: Science and mission overview, *Space Sci. Rev. 79*, 11–32, 1997.

Goldman, M.V., et al., Nonlinear two-stream instabilities as an explanation for auroral bipolar wave structures, *Geophys. Res. Lett., 26*, 1821–1824, 1999.

Gurnett, D.A., et al., The wide-band plasma wave investigation, *Space Sci. Rev., 79*, 195–208, 1997.

Gustafsson, G., et al., The Electric Field and Wave Experiment for the Cluster Mission, *Space Sci. Rev., 79*, 137–156, 1997.

Lucek, E.A., et al., Cluster magnetic field observations at a quasi-parallel bow shock, *Ann. Geophys., 20*, 1699–1710, 2002.

Mangeney, A., et al., WIND observations of coherent electrostatic waves in the solar wind, *Ann. Geophys., 17*, 307–320, 1999.

Mann, G., et al., Statistical analysis of short large-amplitude magnetic structures in the vicinity of the quasi-parallel bow shock, *J. Geophys. Res., 99*, 13315–1323, 1994.

Matsumoto, H., et al., Electrostatic solitary waves (ESW) in the magnetotail: BEN wave forms observed by GEOTAIL, *Geophys. Res. Lett., 21*, 2915–2918, 1994.

Muschietti, L., et al., Phase-space electron holes along magnetic field lines, *Geophys. Res. Lett., 26*, 1093–1096, 1999.

Mozer, F.S., et al., New features of time domain electric-field structures in the auroral acceleration region, *Phys. Rev. Lett., 79*, 1281–1284, 1997.

Omura, Y., et al., Electron beam instabilities as generation mechanism of electrostatic solitary waves in the magnetotail, *J. Geophys. Res., 101*, 2685–2697, 1996.

Pedersen, A., et al., Four-point high time resolution information on electron densities by the electric field experiment (EFW) on Cluster, *Ann. Geophys., 19*, 1483–1489, 2001.

Schwartz, S.J., and Burgess, D., Quasi-parallel shocks: A patchwork of three-dimensional structures, *Geophys. Res. Lett., 18*, 373–376, 1991.

Schwartz, S.J., et al., Observations of Short Large-Amplitude Magnetic Structures at a quasi-parallel shock, *J. Geophys. Res., 97*, 4209–4227, 1992.

Temerin, M., et al., Observations of double layers and solitary waves in the auroral plasma, *Phys. Rev. Lett., 48*, 1175–1179, 1982.

Tsurutani, B.S., et al., Plasma waves in the dayside polar cap boundary layer: Bipolar and monopolar electric pulses and Whistler mode waves, *Geophys. Res. Lett., 25*, 4117-4120, 1998.

M. André, R. Behlke, Swedish Institute of Space Physics, Uppsala division, Box 537, 75121 Uppsala, Sweden. (mats.andre@irfu.se, rico.behlke@irfu.se)

S.D. Bale, Space Science Laboratory, University of California, MC 7450, Berkeley, CA 94720, USA. (bale@ssl.berkeley.edu)

A. Balogh and E.A. Lucek, Space and Atmospheric Physics Group, Blackett Laboratory, Imperial College, London, SW7 2BW, UK. (a.balogh@ic.ac.uk, e.lucek@ic.ac.uk)

C.A. Cattell, School of Physics and Astronomy, University of Minnesota, Tate Lab, 116 Church Street S.E., MN 55455 Minneapolis, USA. (cattell@belka.space.umn.edu)

A.N. Fazakerley, Mullard Space Science Laboratory, University College London, Holmbury St. Mary, Dorking, Surrey RH5 6NT, UK. (anf@mssl.ucl.ac.uk)

J.S. Pickett, Space Plasma Wave Group, Department of Physics and Astronomy, University of Iowa, Iowa City, IA 52242, USA. (pickett@uiowa.edu)

(Received _____.)